

1 **OxyMES. A combination of oxy-fuel technology and microbial**
2 **electrosynthesis for sustainable energy storage**

3 **Ruth Diego-García^{a c}, Antonio Morán^a, Luis M. Romeo^b**

4
5 ^a Chemical and Environmental Bioprocess Engineering Group, Natural Resources Institute (IRENA),
6 Universidad de León, Av. Portugal, 41, 24009 León, Spain

7 ^b School of Engineering and Architecture, Department of Mechanical Engineering, Universidad de Zaragoza,
8 Campus Río Ebro, María de Luna 3, 50018, Zaragoza, Spain

9 ^c Fundación Ciudad de la Energía (CIUDEN), Cubillos del Sil (León), Spain

10
11
12 **ABSTRACT**

13 Advances in renewable energy generation technologies entail the necessary deployment of
14 associated energy storage technologies. One of them is *power-to-gas* technology, which
15 make use of the surplus electricity from the system for its conversion and storage in the
16 form of synthetic natural gas. These systems enable to convert the current fossil fuel-based
17 gas system into a system that operates with biological origin gases (bioenergy). In this
18 context, locally generated *power-to-gas* schemes based on biological subprocesses are of
19 great interest. Microbial electrosynthesis (*MES*) cells are biological systems that produce
20 biogas via microbial action and the supply of electrical energy. The *MES* subsystem can be
21 integrated as a fundamental part of an energy storage and utilization system. The *OxyMES*
22 scheme proposed is a *power-to-gas* system that seeks to neutralize the emissions of a
23 standard industrial process through the hybridization of oxy-fuel combustion and
24 bioelectrochemical processes. The energy balance analysis yielded a *power-to-gas*
25 efficiency in the *MES* cell close to 51% and a global performance of the *OxyMES*
26 integrated system close to 60%, for a cell with a faradaic efficiency of 80%, CO₂-to-CH₄
27 conversion rate of 95% and $\Delta V_{\text{cell}} = 1.63$ V.

28
29
30
31
32
33 **Keywords:** Power to Gas; renewable energy surplus; CO₂ conversion; energy storage;
34 biogas; oxycombustion, microbial electrosynthesis; hybrid and integrated processes.

35 Corresponding author's (*): +34 987 291 841

36 e-mail address: amorp@unileon.es (A. Moran); rdiegg00@estudiantes.unileon.es (R.
37 Diego)

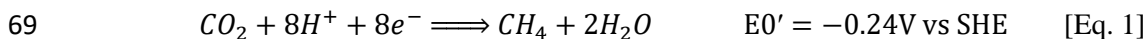
38 1. INTRODUCTION

39 According to the IEA, the *net-zero emissions* target for 2050 is to achieve a 45% reduction
40 in total CO₂ emissions by 2030 compared 2010 [1]. The Paris Agreement and European
41 recent commitments also force to implement an important increase of the contribution of
42 renewable energy sources (RES) for the next years. In the case of EU of at least 40% of the
43 final gross energy consumption [2, 3, 4].

44 For the rapid implementation of renewable energies in the electrical system to be viable,
45 they need to be deployed alongside energy storage technologies that enable their
46 integration into the electrical system, minimizing the electricity surplus and ensuring the
47 operability of the system [5, 6]. *Power-to-gas* technologies (PtG), which make use of the
48 renewable electricity surplus of the system for storing it in the form of gas through
49 electrolysis [7, 8], is a sound alternative for energy storage. It allows the interconnection
50 and transfer of energy between the electrical and the gas systems [9, 10], providing both
51 with the possibility of increasing their capacity factor and flexibility and improving their
52 ability to adapt to demand, expanding the profitability options by participating in other
53 electricity market services [11].

54 Moreover, in 2016, emissions from energy use in industry accounted for 24.2% of the total
55 of 49.4 GtCO_{eq} [12]. Certain carbon-based industries will need to adapt their processes to
56 neutralize them. The *power-to-gas* systems allow converting the current fossil fuel-based
57 gas system into a system that operates with biologically derived gases generated with
58 renewable sources, thus getting closer to a more environmentally sustainable energy model
59 and circular economy [13, 14, 15].

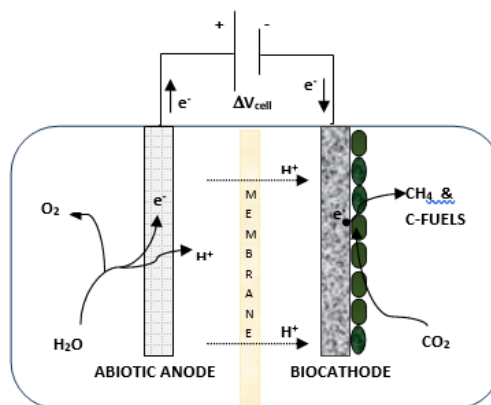
60 In this context, local generated *power-to-gas* schemes based on biological subprocesses
61 have been identified as being of great interest. Among them, one of the most promising
62 options for converting electrical energy surplus is the use of microbial systems. Microbial
63 electrosynthesis (*MES*) cells are biological systems that produce biogas as a result of
64 microbial action and the supply of electrical energy. They are based on the fact that some
65 microorganisms, such as methanogens, have the natural ability to use CO₂ to produce
66 organic compounds [16]. It has been found that genera such as *Geobacter*, *Clostridium* and
67 *Sporomusa* act as biocatalysts by accepting electrons from a solid electrode to reduce CO₂
68 directly or indirectly into organic compounds such as methane [17], according to Eq. 1:



70 The transfer of electrons between microbes and electrodes can be via direct electron
71 transfer (DET), indirect (IET) or through soluble electron acceptors acting as mediators
72 (MET) [17, 18, 19]. The ability of microorganisms to produce methane from reducing CO₂
73 by using an electrode acting as a direct electron donor was first referenced by Cheng et al.
74 [20]. During the electrochemical interactions of the cathode, hydrogen is produced, either
75 by bioelectrochemical processes of certain microorganisms or by electrolysis reactions
76 when applying a potential in the cathode immersed in an aqueous electrolyte. Hydrogen
77 can act as an electron donor in CO₂ reduction reactions, thus promoting indirect electron
78 transfer (IET). Depending on the potential applied to the cathode, one of the electron

79 transfer mechanisms (DET vs. IET) is favoured, although this parameter also influences
80 the methane production obtained [17]. Villano et al. [19] and Gomez et al. [21] observed
81 that a biocathode improves current densities compared to an abiotic cathode that only
82 produces hydrogen.

83 Thus, *MES* cells mainly consist of two electrodes (anode and cathode) immersed in an
84 electrolyte (water) and an electroactive biofilm on the cathode (biocathode) with
85 microorganisms that electrocatalyse the CO₂ reduction reaction. A proton-exchange
86 membrane (PEM) is also used to separate the anodic and cathodic chambers. The electrode
87 in the anodic chamber is usually a mesh or sheet of some metallic material, such as Ti/IrO₂.
88 Fig. 1 shows a basic diagram of an *MES* cell.



89

90

Fig. 1. Schematic representation of MES. Adapted from Bajracharya, et al [17]

91 The *MES* system can be integrated as a fundamental part of an energy storage and
92 utilization system. The *OxyMES* scheme proposed below is a *power-to-gas* system that
93 seeks to neutralize the emissions of an industrial process through the hybridization of oxy-
94 fuel combustion and bioelectrochemical processes. In this work, the integrated operation of
95 units that work in oxy-fuel mode is studied to achieve the capture and conversion of their
96 CO₂ emissions that, until now, have not been analysed jointly. There are references of
97 studies of hybridization schemes of oxyboilers, clinker kilns and MSW incinerator in
98 *power-to-gas* systems, [22], [23], [24], [25], all of them based on industrial systems of
99 non-biological origin. In the *P2G-BioCat* project [26], hydrogen from an electrolyzer and
100 CO₂ are methanized by microorganisms in a biological reactor; the biomethane produced is
101 injected in the gas grid [27].

102 The design of the *OxyMES* system has been developed as a result of searching for
103 emissions neutralization in industries that carry out oxy-fuel combustion processes. The
104 use of these emissions in biological systems that convert them into products with an
105 energetic value (biogas) is pursued. Certain designs of *MES* cells, such as the one
106 proposed, allow obtaining pure oxygen as a byproduct in the anodic chamber, which is
107 precisely what is used in the boiler during the oxycombustion [28].

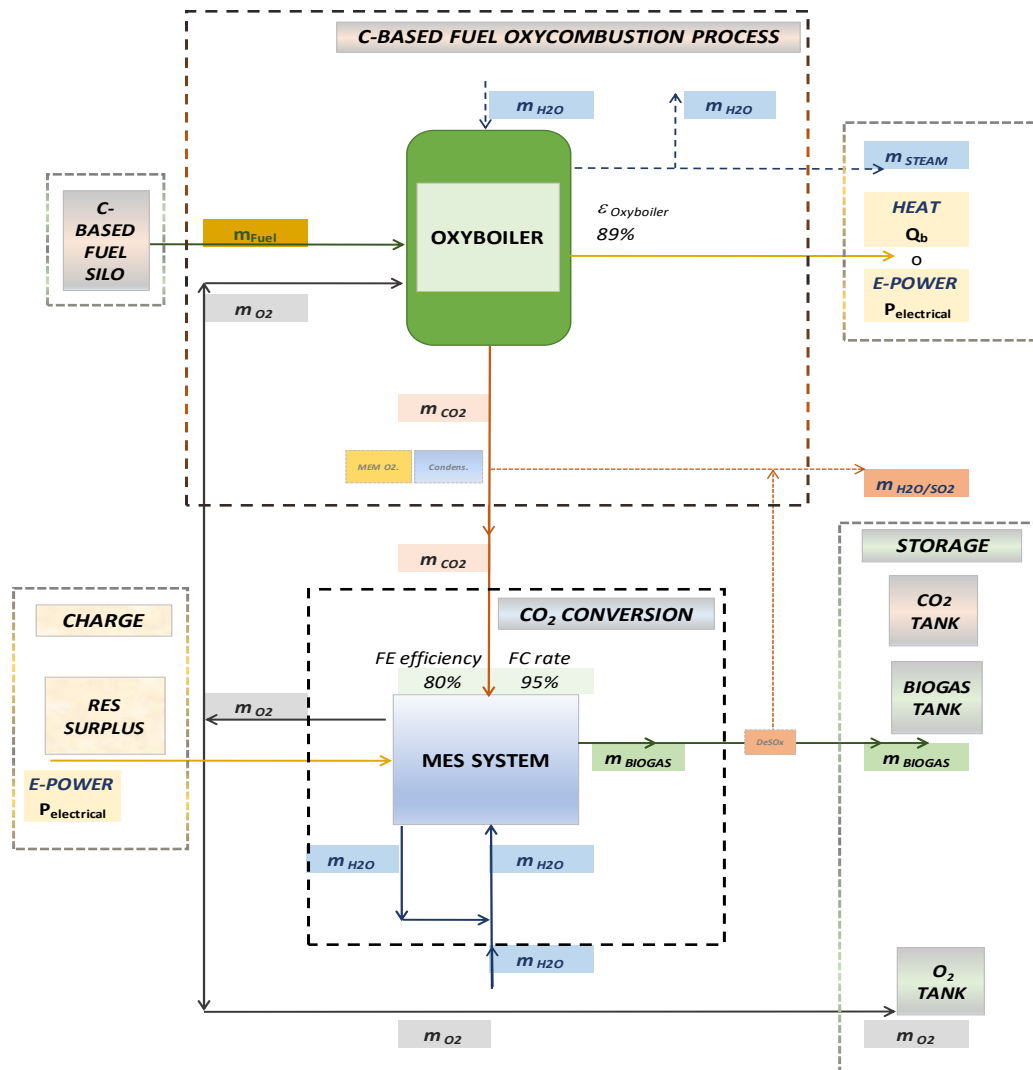
108 This work presents the concept and the basic sizing of the main necessary equipment.
109 Although the technological development of the *MES* cell is less advanced than the rest of
110 the proposed processes, the study shows the potential of this technology when its

111 development accelerates and its technology readiness level (TRL) increases. The
 112 integration of conventional energy production systems (boilers) with novel bio-based
 113 systems (microbial electrosynthesis cells) presumes the main challenges to be addressed in
 114 this type of hybrid schemes.

115

116 **2. DESCRIPTION OF THE PROPOSED PROCESS: OXYMES**

117 The process integrates an oxycombustion plant (oxyboiler) with a microbial
 118 electrosynthesis system (MES). The diagram of the proposed process is schematically
 119 illustrated in Figure 2. The process combines the use of renewable electricity surplus with
 120 the capture of CO₂ emissions generated in industrial processes through the integration of
 121 biomethanization and oxy-fuel combustion processes. With this, it is possible to store the
 122 electricity surplus in the form of a biogas for its subsequent storage and delivery to the
 123 natural gas network or any other use.



124

125 **Fig. 1.** Basic scheme for novel process proposed 'OxyMES', integrated by three main sub-units: Oxyboiler,
 126 MES cell and tanks system (boundary limits marked in dashed lines).

127 The oxy-fuel boiler provides gases with a high concentration of CO₂ to the *MES* cell while
128 generating steam for heating purposes and/or electricity production. In the cathodic
129 chamber of the *MES* cell, CO₂ is converted into CH₄ which, together with the rest of the
130 minor compounds of the oxycombustion gas stream, form what we will call *biogas*.
131 Likewise, the anodic chamber produces a stream of pure oxygen that is used in the boiler
132 for oxy-fuel combustion, thus avoiding the air separation unit (ASU), present in the typical
133 designs for this type of industry [29].

134 The CO₂ gases from the industrial oxy-fuel combustion process are thus recovered as
135 methane, forming a biogas fuel that can be totally or partially injected into the network
136 once its composition has been adjusted to the quality requirements of the gas system [30].
137 The system includes oxygen storage tanks and biogas.

138

139 **2.1. Oxyfuel boiler**

140 The study is based on the design of a semi-industrial demonstration plant, which has a
141 pulverized coal boiler with a nominal power of 20 MW_{th}, as well as the rest of the auxiliary
142 systems necessary for its operation (preparation fuel train, oxidizers, etc.). This plant is
143 located in the Technology Development Center of the *Fundación Ciudad de la Energía*
144 (CIUDEN), located in Cubillos del Sil (León, Spain) [31]. The operating data of the
145 oxycombustion plant were obtained during the tests carried out in the framework of the
146 FP7 European co-funded project, *RELCOM* Project [32]. The experimental tests used
147 bituminous coal of South African origin, whose characteristics are reflected in Table 1 of
148 supplementary material. The plant performed tests both in conventional combustion with
149 air as oxidizer, as well as in oxycombustion mode with different degrees of flue gases
150 recirculating towards the boiler, mixed with pure oxygen (> 99.5% purity) supplied from
151 cryogenic liquefied oxygen tanks.

152

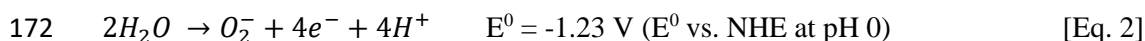
153 **2.2. MES system**

154 In the *OxyMES* scheme, the inlet flows to the cathodic chamber of the *MES* cell are the
155 combustion gases produced in the oxyboiler, the make-up water for the *MES* cell and the
156 electricity to maintain the potential between the electrodes, which will come from the RES
157 surpluses. Oxycombustion gases are mainly composed of CO₂, water vapour and N₂. The
158 outlet streams of the *MES* cell, in the form of products, are a stream of high purity oxygen
159 produced in the anode and another of biogas with a methane concentration greater than
160 50% by weight, produced in the cathode. Part of the oxygen produced in the *MES* cell is
161 introduced into the oxyboiler to perform oxycombustion and replace the ASU oxygen
162 supply. The remaining oxygen is stored in the tank.

163 *MES* systems, designed from the perspective of *power-to-gas bioelectrochemistry*
164 (BEP2G), combine the production of energy carriers (CH₄) with the sequestration of CO₂
165 [21, 33]. The model that simulates what happens inside the *MES* cell considers that the
166 oxygen evolution reaction (OER) that generates molecular oxygen (O₂) takes place at the

167 anode. Meanwhile, in the cathode, CO₂ is reduced to organic compounds due to the
168 catalytic action of microorganisms. The protons (H⁺) cross the membrane separating the
169 two half-cells from the anodic chamber to the cathodic chamber. The redox half-reactions
170 are:

171 *Anode half-reaction:*



173 *Biocathode half-reaction:*



175 where E⁰ are the standard potentials related to CO₂ reduction and water oxidation with
176 reference to Normal Hydrogen Electrode (NHE) at pH=0.

177 The process requires the contribution of energy from an external source, in the form of
178 electrical energy, through the application of a potential to the electrodes, sufficient to
179 trigger the reduction–oxidation reactions (redox) and overcome the losses of the process
180 itself. This external energy will come from the surpluses of the electrical system. One of
181 latest published works of *MES* cells designed for the simultaneous production of oxygen in
182 the anode and methane in the cathode [21] uses a cell in which the potential applied
183 between anode and cathode is 2.8 V. In addition, it should be noted that there are studies in
184 which it has been shown that microorganisms are still active after an electricity supply
185 interruption [34].

186 As seen in the redox half-reaction (Eq. 3), for the reduction of 1 mole of CO₂ to methane, 8
187 moles of electrons are needed, which implies that the gas flow to be treated from the
188 oxyboiler stream involves a higher number of electrons to transfer through the external
189 electrical circuit of the electrochemical cell compared to what would be required to
190 produce other compounds such as hydrogen (supplementary material). Both the redox
191 potential of the electrode and the pH of the electrolyte influence the species obtained in the
192 cell [17].

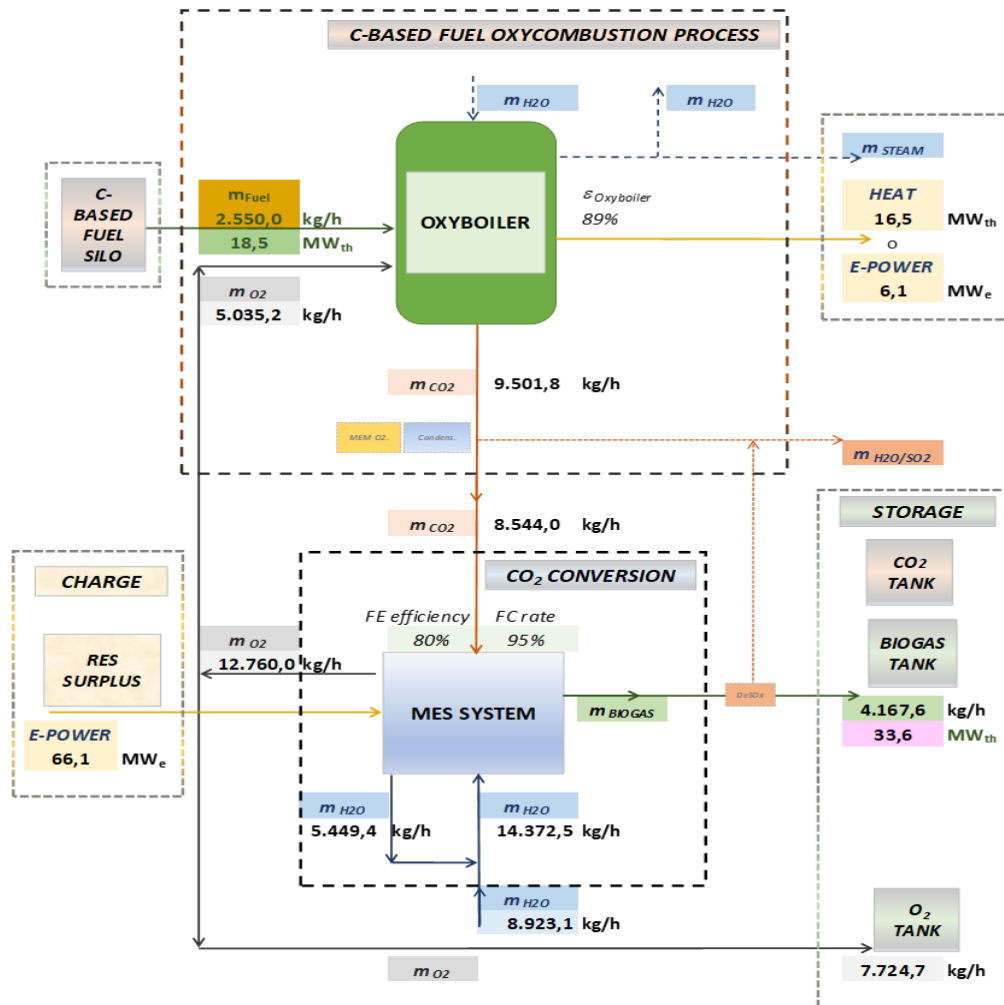
193 Regarding electrode potentials, Villano et al. [19] observed that methane was produced in
194 cathodic potentials more negative than -0.7 V (vs. Ag/AgCl), which corresponds to -0.5
195 vs. SHE at pH 7, and at -0.8 vs. SHE, the efficiency in the conversion of electrical current
196 into methane reached 96%. Later, Villano et al. [35] reported methane production of 9.7 ±
197 0.6 mmol/l day in a two-chamber *MEC* cell, with a conversion efficiency of electrical
198 current to methane of 84-90% and a conversion efficiency of acetate to current at the anode
199 of 72-80%. The cathodic efficiency in methane production in most studies reaches 95-99%
200 with biocathode potentials between -0.7 V and -0.8 V vs. SHE, [17]. Similarly, Batlle-
201 Vilanova [36] reported a biocathode potential of -0.8 V vs. SHE, obtaining a faradaic
202 conversion of 89.7% and a conversion ratio of CO₂ to methane of 95.8%. Gómez et al. [21]
203 recently demonstrated the continuous production of methane in a cell with and without a
204 membrane with a cathode potential between -0.9 V and 0.7 V vs. NHE, with an average
205 cathodic efficiency of 84%.

206 In addition, in the *MES* cell during microbial electrosynthesis, a certain amount of thermal
 207 energy is produced that can be used in another part of the process. In this study, it was
 208 considered negligible.

209

210 2.3. Integrated process. Balance of Plant (BOP)

211 Fig. 3 identifies the main streams of the study. The gas stream to be introduced into the
 212 *MES* cell is taken from the outlet of the dust particle filter of the oxycombustion plant,
 213 normally set at 180 °C. At this point, the flue gases have the composition shown in Table
 214 1. The flow and composition values of the fuel and the flue gases leaving the
 215 oxycombustion plant are obtained from the experimental tests performed in the reference
 216 demonstration plant [31], Table 1. The model is simulated by performing the mass and
 217 energy balances of each of the process streams. In this study, a base case of oxyboiler
 218 operation is considered, feeding 2550 kg/h of bituminous coal with the characteristics
 219 shown in supplementary material. This operational scenario remains fixed for the entire
 220 study, so that the flow rate of oxycombustion gases entering the *MES* cell is also constant
 221 for all cases and, therefore, the biogas produced.



222

223 Fig. 3. Conceptual layout of the analysed OxyMES system, including main mass and energy flow data.

	Oxyboiler plant outlet (%w _{th} , w.b.)	MES cell inlet (%w _{th} , w.b.)	MES cell outlet (%w _{th} , w.b.)
CH ₄	-	-	57.96
CO ₂	73.79	82.06	8.39
H ₂ O	10.38	2.91	2.91
N ₂	11.56	12.86	26.29
O ₂	3.54	1.57	3.22
SO ₂	0.33	0.15	0.30
Ar	0.40	0.45	0.92

225 **Table 1.** Flue gases composition at oxyboiler plant outlet and biogas composition at inlet/outlet of the
226 *MES cell.*

227 To avoid affecting the microorganisms of the *MES* cell, the temperature of the gas stream
228 is set at 32 °C [37]. In addition, since the process must be anaerobic, the oxygen content is
229 limited to a maximum of 2% by volume in the flue gas stream, however there are recent
230 studies that indicate the possibility of reaching higher values, although methane production
231 is reduced [38]. Staying oxygen below 2%_{vol} involves incorporating a gas conditioning
232 train ahead of the cell for cooling and condensing its moisture as well as part of the SO₂
233 and O₂ content. If in practice the oxygen content requirement is not met, a dedicated
234 equipment (deOxo or similar) should be included to ensure this condition (out of the scope
235 of this work). According to calculations, the biogas generated in the *MES* cell has the
236 composition shown in Table 1.

237

Oxyboiler plant inlet/outlet	MES cell inlet/outlet
Fuel (pulverized coal) flow, m _f : 2.55 t/h	Oxycombustion flue gases flow: 8.5 t/h **
LHV _{fuel} : 26137 kJ/kg	CO ₂ flow (contained in oxy-flue gases): 7.0 t/h
Input thermal power, LHV, P _{in} : 18.5 MW _{th}	O ₂ content in oxy-flue gas: < 2% _{vol}
Oxyboiler thermal efficiency, LHV, μ _{oxyboiler} : 89%	Net water consumption: 8.9 t/h
Output thermal power, LHV, P _{out} (Q _b): 16.5 MW _{th}	Electrical power consumption: 66.1 MWe ***
Oxygen flow (fresh): 5.0 t/h	Biogas flow, m _{biogas} : 4.17 t/h
Oxycombustion flue gases flow: 9.5 t/h ;180 °C *	CH ₄ flow (contained in biogas), F _{CH4} : 2.4 t/h
	LHV _{CH4} : 50000 kJ/kg
	Biogas power, LHV: 33.64 MW
	Faradaic efficiency, FE: 80%
	CO ₂ -to-methane conversion rate, FC: 95%
	Operational temperature: 30-35 °C

238 **Table 2.** Main technical characteristics for units and subunits. Simulation assumptions and operational
239 parameters for sizing main units OxyMES system.

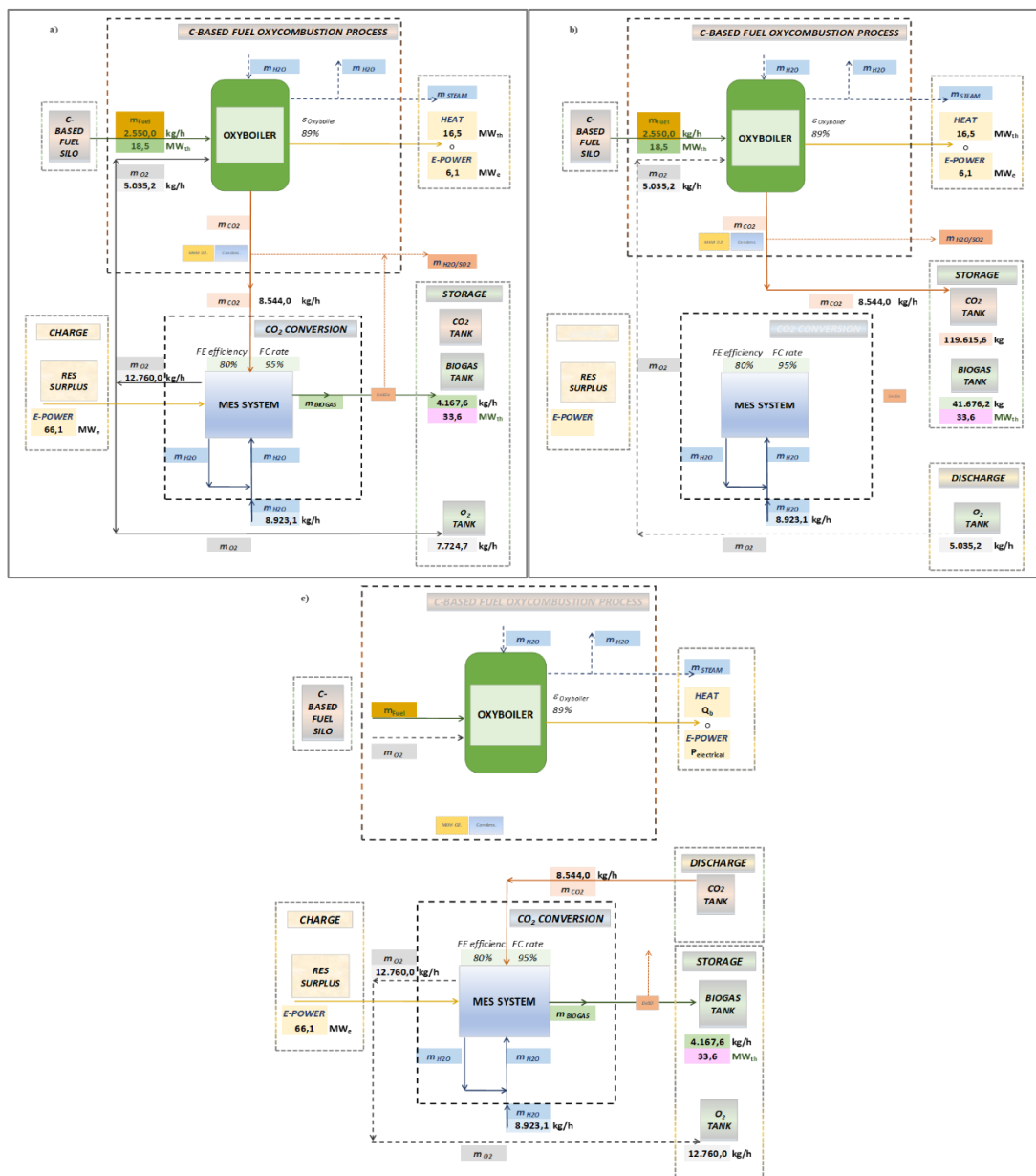
240 * Oxycombustion flue gases at oxyboiler plant outlet, after recirculation (before stack).

241 ** Oxycombustion flue gases after water condensation, at MES cell inlet.

242 *** The electrical power input for the MES is calculated considering ΔV_{cell}: 1.63 V, FE: 80%; FC: 95%.

243 The energy stored by the *OxyMES* is a function of the operating hours of the
 244 aforementioned system and these, in turn, of the storage tank capacity of the biogas
 245 produced in the *MES* cell. Initially, the design assumes that these operation hours will
 246 correspond to the number of hours in which the renewable electricity surpluses are
 247 produced, although this is a criterion that can vary according to the final application and
 248 the degree of autonomy sought. In this case, 10 hours of *MES* cell operation have been
 249 considered, with which the chemical energy stored in the form of biogas is 336 MWh_{th}. In
 250 turn, the operation of the oxyboiler is directly conditioned by the capacity of the oxygen
 251 tank, since this must be sufficient to cover the hours that the plant is in operation. In short,
 252 the system of tanks for storage of process fluids is a key element that directly affects the
 253 operation of the whole and must be properly designed so that they meet the expected stored
 254 energy (MWh) and autonomy objectives of the plant.

255



256

257 **Fig. 4.** Charge, discharge and storage cycles in the *OxyMES* system standard operation profile. a) *Oxyboiler*
 258 and *MES* are ON: CO₂ from oxyboiler feeds the *MES* cell and it is converted to biogas and stored during a

259 *RES surplus period (RES charge, biogas and O₂ storage); b) Oxyboiler ON and MES OFF: CO₂ from*
 260 *oxyboiler is led to its storage tank during high-demand periods with no RES surplus; O₂ is fed to the*
 261 *oxyboiler to maintain the oxycombustion (CO₂ charge, O₂ discharge); c) Oxyboiler OFF and MES ON:*
 262 *during oxyboiler shutdowns when RES surplus occurs, CO₂ from tank feeds the MES cell to convert it into*
 263 *biogas (RES charge, CO₂ discharge, biogas and O₂ storage).*

264

265 The *OxyMES* system can be parameterized as an energy storage one: 33.6 MW/336 MWh.
 266 Without going into detail considerations, the capacity and autonomy of the CO₂ tank are
 267 the parameters that will define the maximum power of the *OxyMES* system (33.6 MW),
 268 while the capacity of the biogas tank is the stored energy (336 MWh).

269 To size the complete *OxyMES* system, we begin by defining a daily operating profile of the
 270 *MES* cell considering that it operates during the hours in which the RES surpluses occur.
 271 For this work, an average of 10 h per day concentrated in the central hours of the day has
 272 been considered [39]. This assumption has been made by analysing the expected
 273 *oversupply* of renewable energies in scenarios projected to 2030 with high penetration of
 274 renewable energies (mainly solar and wind) and without storage systems (Fig. 5). It is
 275 during the operation of the *MES* cell that the biogas produced and the oxygen left
 276 unconsumed in the oxyboiler will be stored. Therefore, the oxygen stored during the
 277 charging process (Fig. 4.a) must be sufficient to cover the oxygen consumption of the
 278 oxyboiler during the next period, in which the *MES* cell is no longer coupled to the
 279 oxyboiler because there is no renewables surplus (Fig. 4.b). The final capacity of the tank
 280 system will depend on the hourly, daily or even weekly scope, defined by the operator of
 281 the industry or, in other words, the stored energy (MWh) that is to be made available to the
 282 system.

283

MES cell, inlets streams (consumptions)	
Oxyboiler flue gas flow after cooling, kg/h	8544
CO ₂ flow (contained in oxy-flue gas) after cooling, kg/h	7011
Water net flow, kg/h	8923
(RES) Electrical power, MWe	66
MES cell outlets streams (products)	
Raw biogas flow, kg/h	4178
Methane flow (contained in the biogas flow), kg/h	2422
Oxygen flow, kg/h	12760

284 **Table 3.** Hourly flows of CO₂ consumed and oxygen and biogas produced in the *MES* cell from the mass
 285 balance calculations.

286

287

288

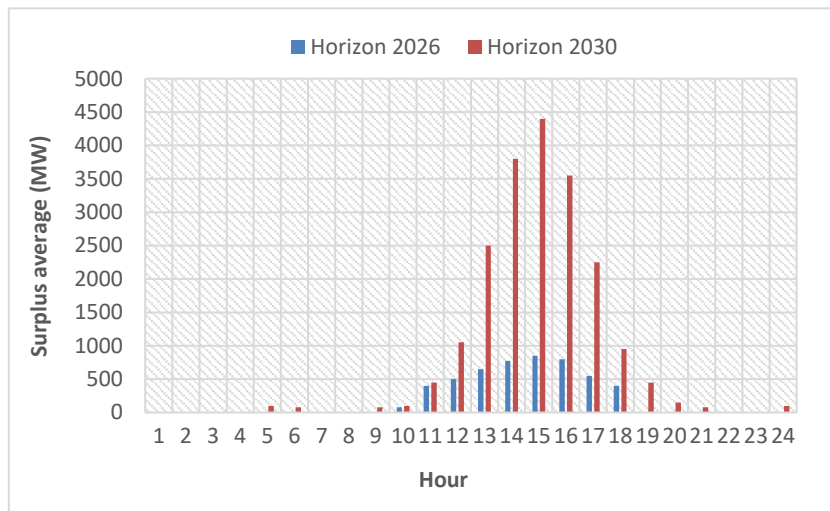
289

290

MES cell, 10-hour operation profile	
Biogas stored*, kg//tank autonomy, h	41676//10 h
Biogas chemical energy stored, MWh _{th}	579
Oxygen store, kg//tank autonomy, h	77247//10 h
Oxygen net store (stock), kg	6754
CO ₂ store, kg//tank autonomy, h	119615//14 h

291 **Table 4.** Minimum capacity of CO₂, O₂ and biogas tanks for 10 hours of MES cell operation. * Note: biogas
 292 is stored after a deSO_x treatment (Fig. 3).

293



294

295 **Fig. 5.** Pattern of hourly oversupply associated with photovoltaic (PV) production in Spain (central hours of
 296 the day). In 2030, it will be able to reach values above 4000 MW. Adapted from [5]

297

298 **2.4. Analysis of partial performance and global performance of the OxyMES hybrid** 299 **process**

300 To evaluate the *OxyMES* process, the efficiency of the two main subsystems (oxyboiler
 301 and *MES* cell) that make up the hybrid system has been defined. These performances are
 302 calculated by the relationship between the energy produced and the energy supplied to
 303 operate the subsystem, according to their respective boundary limits (black dashed lines in
 304 Fig. 3). Then, the global *OxyMES* system performance can be obtained.

305 The thermal energy generated in the oxyboiler Q_b (MW_{th}) is a function of the performance
 306 of the oxycombustion boiler, $\mu_{oxyboiler}$, which has been calculated from the experimental
 307 data gathered in [32], resulting in an average value of 89% LHV basis, which is close to
 308 that reported in various studies on oxyfuel power plants (> 87.37% HHV, [29]; > 90% -
 309 93% LHV, [40]). This Q_b is the thermal energy of the steam produced and it is available
 310 for thermal uses of the plant or for its conversion to electrical energy through a Rankine
 311 cycle in a steam turbine.

$$312 \mu_{Oxyboiler, LHV \text{ basis}} (\%) = \frac{Q_b \text{ Oxyboiler}}{LHV_f \cdot \dot{m}_f} \times 100 \quad [\text{Eq. 4}]$$

313 In relation to the *MES* system, the electrical energy consumed comes from the *RES* surplus
 314 of the network. This is used to maintain the potential in the electrodes of the
 315 electrochemical cell, which is necessary to promote the transport of electrons that convert
 316 the CO₂ molecules into CH₄ ones. In turn, the chemical energy of the methane produced in
 317 the biocathode, E_{biogas}, can be considered as energy produced by the *MES* cell. The
 318 **electrical energy consumed** in the *MES* cell, required to reduce the CO₂ to methane, is:

$$319 \quad E_{MES} = \Delta V_{cell} \cdot I \quad [\text{MJ/tCH}_4] \quad [\text{Eq. 5}]$$

320 where ΔV_{cell} is the external applied voltage to the cell and I is the current intensity
 321 calculated as the specific flow of electrons from the anode to the cathode through the
 322 external electrical circuit.

$$323 \quad \Delta V_{cell} = \Delta V_{\text{theoretical cell}} + E_{\text{overpotentials}} = E^0_{\text{cathode}} - E^0_{\text{anode}} + E_{\text{overpotentials}} \quad [\text{V}] \quad [\text{Eq. 6}]$$

324 Due to the losses of the electrochemical process in both electrodes, $E_{\text{overpotential}}$, it is
 325 necessary to apply a potential ΔV_{cell} greater than that theoretically necessary according to
 326 the thermodynamics of the global redox reaction, with $\Delta V_{\text{theoretical cell}} = E^0_{\text{cathode}} - E^0_{\text{anode}} =$
 327 $0.169 - (-1.23) = -1.06 \text{ V vs. NHE, pH 0}$ [Eq. 7], where E^0 are the standard potentials of
 328 the electrodes. The negative sign indicates that the reaction is not spontaneous.

329 To obtain the efficiency of the global microbial electrosynthesis process in the cell, the
 330 actual conversion of CO₂ to methane (FC or CO₂-to-CH₄ ratio) must be considered, thus
 331 expressing the carbon captured and converted into product. It is also necessary to consider
 332 a factor that indicates the efficiency in the electrical conversion towards that product, in the
 333 electrodes (mainly, cathode) of the cell (faradaic efficiency, FE) [36]. With these
 334 parameters, the specific flow of electrons per ton of methane produced, I , is calculated
 335 (Fig. 1):

$$336 \quad I = (n_{CO_2} \cdot n \cdot F \cdot 100 / FE) \cdot (M_{CO_2} / M_{CH_4}) \cdot (100 / FC) \quad [\text{C/tCH}_4] \quad [\text{Eq. 8}]$$

337 where n_{CO_2} , is moles of CO₂/tCO₂, n is moles of electrons per mole of CO₂-to-CH₄, F is the
 338 Faraday constant, 96485 C/mol e⁻, and M is the molecular weight. The electrical power
 339 consumed by the *MES* cell is:

$$340 \quad P_{e_MES} = E_{MES} \cdot F_{CH_4} \quad [\text{MW}] \quad [\text{Eq. 9}]$$

341 where F_{CH_4} is the methane flow rate in t/h produced in the *MES* cell. The supplementary
 342 material includes the development of the calculation to obtain the specific current intensity,
 343 I , and the electrical consumption E_{MES} in the *MES* cell.

344 In experimental studies, it has been found that to achieve interesting results in the
 345 operating parameters of the cells, the potential applied to the cell (ΔV_{cell}) varies, in
 346 practice, between values close to 4 V [41] and 2.6 V [21], although it is expected to be able
 347 to reduce these values to approximately 1.7 V, in view of the lower value of biocathode
 348 potential reported thus far (-0.4 V vs. SHE) by Beese-Vasbender et al. [42], which also
 349 reached a cathodic efficiency of 80%.

350 Based on the bibliographic references [17] and [21], for the calculation of the electrical
 351 consumption of the *MES* cell in this study, a faradaic efficiency value, FE, of 80% and a

352 CO₂ to methane conversion factor, FC, of 95% were used. Applying the previous
 353 equations, the results of the electrical power consumed, P_{e_MES}, are presented in Table 5 for
 354 four assumptions of the external applied voltage ($\Delta V_{cell} = 1.23 \text{ V}, 1.63 \text{ V}, 2.8 \text{ V}$ and 3.5
 355 V).

356 With all of the above, the energy efficiency of the *power-to-gas* conversion is calculated in
 357 the *MES* cell (μ_{PtG_MES}) as the ratio between the energy obtained in the form of chemical
 358 energy from biogas (E_{biogas}) and the electrical energy supplied to produce the
 359 aforementioned biogas (E_{MES}):

$$360 \mu_{PtG_MES}(\%) = \frac{E_{biogas}}{E_{MES}} \times 100 = \frac{LHV_{CH_4} \cdot \dot{m}_{CH_4}}{\Delta V_{cell} \cdot I} \times 100 \quad [\text{Eq. 10}]$$

361 The value obtained from this *power-to-gas* efficiency, μ_{PtG_MES} , for the case $\Delta V_{cell} = 1.63 \text{ V}$
 362 is 50.88%, as shown in Table 5.

363 Finally, once the energy balances are performed for each subunit, the **global efficiency of**
 364 **the oxyMES process** is calculated ($\mu_{PtGtHeat_OxyMES}$) taking as inputs to the boundaries of
 365 the global system, the chemical energy contained in the oxyboiler fuel ($LHV_f \cdot \dot{m}_f$) and the
 366 electrical energy that feeds the *MES* cell (E_{MES}) and, as outputs, the thermal energy of the
 367 steam produced in the oxyboiler (Q_{bOxyBoiler}) and the chemical energy of the biogas (E_{biogas})
 368 generated in the biocathode of the *MES* cell:

$$369 \mu_{PtGtHeat_OxyMES}(\%) = \frac{Q_{bOxyBoiler} + E_{biogas}}{LHV_f \cdot \dot{m}_f + E_{MES}} \times 100 = \frac{Q_{bOxyBoiler} + LHV_{CH_4} \cdot \dot{m}_{CH_4}}{LHV_f \cdot \dot{m}_f + \Delta V_{cell} \cdot I} \times 100 \quad [\text{Eq. 11}]$$

370 If the global performance is calculated for the selected base case of the oxyboiler operation
 371 (18.51 MW_{th} LHV, Table 5, corresponding to the 2550 kg/h of bituminous coal selected)
 372 and an external potential applied in the *MES* cell of $\Delta V_{cell} = 1.63 \text{ V}$, the result obtained is
 373 59.22%, Table 5.

374

375 3. RESULTS AND DISCUSSION

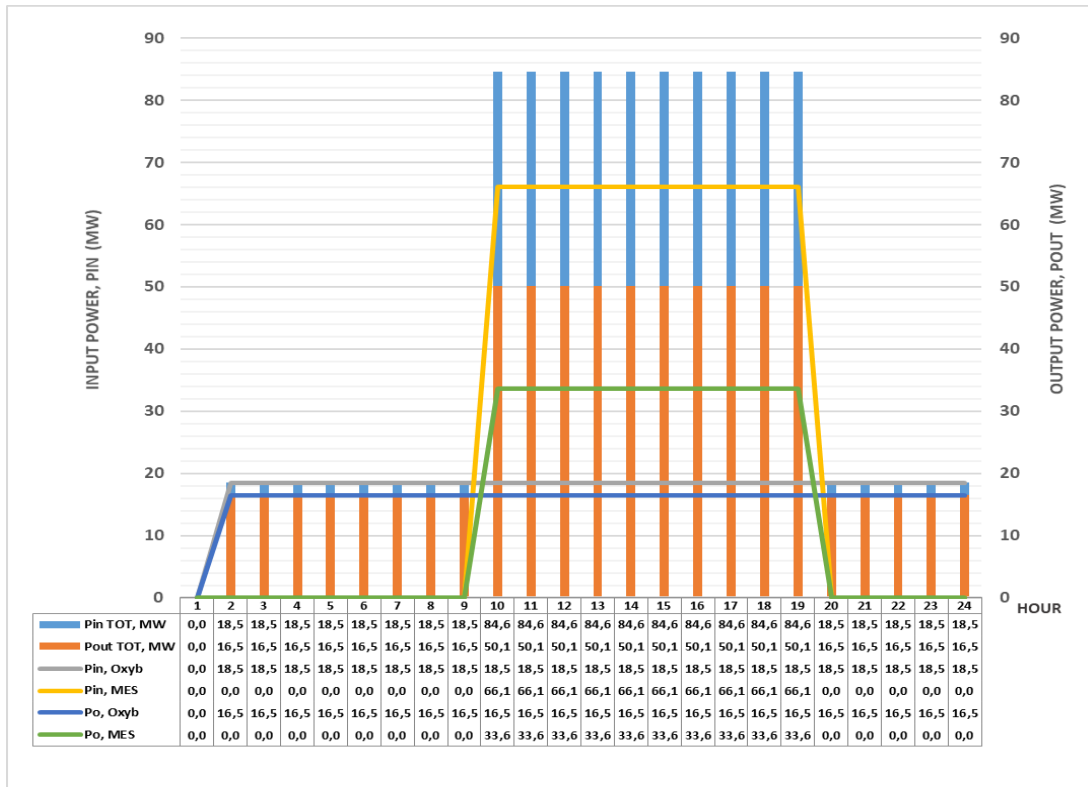
376 3.1. Operating profile

377 As mentioned initially, it has been chosen as basic conditions for the *OxyMES* design that
 378 global emissions are zero and that the system is as self-sufficient as possible. These two
 379 conditions influence the design and sizing of the different main units that make up the
 380 *OxyMES* scheme. The condition of a self-sustaining system necessarily implies the use of
 381 tank storage for the process fluids (oxygen and biogas) and eliminates their external
 382 supplies, especially oxygen. In addition, the tank system allows the transfer of energy in
 383 the successive cycles of charging and discharging to/from the electrical and gas system,
 384 with oxygen acting as *feedstock* and biogas as an *energy carrier*.

385 To carry out these charging and discharging cycles, the oxygen and biogas tanks are sized
 386 so that they can cover the demand of the boiler during the periods in which the *MES* cell is
 387 inactive. In these periods (Fig. 6, 12 am-8 am and 7 pm-12 pm), the oxycombustion gas
 388 stream is stored in its corresponding tank (Fig. 4.b). Table 4 shows the minimum tanks
 389 capacity for 10-hours continuous cell operation. However, the final sizing of the tank

390 system will be determined not only by the duration of the product charging and discharging
 391 cycles but also by its operation profile (continuous/discontinuous) and by the planning of
 392 its final discharge in each cycle of plant operation. We will understand the *cycle of*
 393 *operation* of the plant as the time between two discharges to the external network of the
 394 accumulated stock of oxygen, CO₂ and biogas.

395



396

397 **Fig. 6.** OxyMES daily operation profile. Adjusted to the RES discharge profile in Spain. $P_{in\ TOT}$ (blue) refers
 398 to the total power input (MW) to the global system per hour: sum of chemical coal-fuelled power consumed
 399 by the oxyboiler (grey) and electric power consumed by the MES cell (yellow). $P_{out\ TOT}$ refers to the total
 400 power produced (MW) by the global system per hour: sum of steam heat power (MW) generated in the
 401 oxyboiler (dark blue) and biogas chemical power produced (MW) by the MES cell (green).

402

403 Fig. 7 shows the influence of the operating profile of the plant on the number and size of
 404 the final tanks to be installed. If the discharge cycle is a daily one, the size of the oxygen
 405 storage tank can be optimized by proposing a discontinuous intraday cell operation, Fig. 8.
 406 The greater the time lag between the two start-ups of the MES cell, the lower the required
 407 maximum value of the oxygen tank capacity.

408

409
410
411
412
413
414
415
416
417
418
419
420
421
422
423
424
425
426
427
428
429
430
431
432
433
434
435
436
437
438
439
440
441
442
443

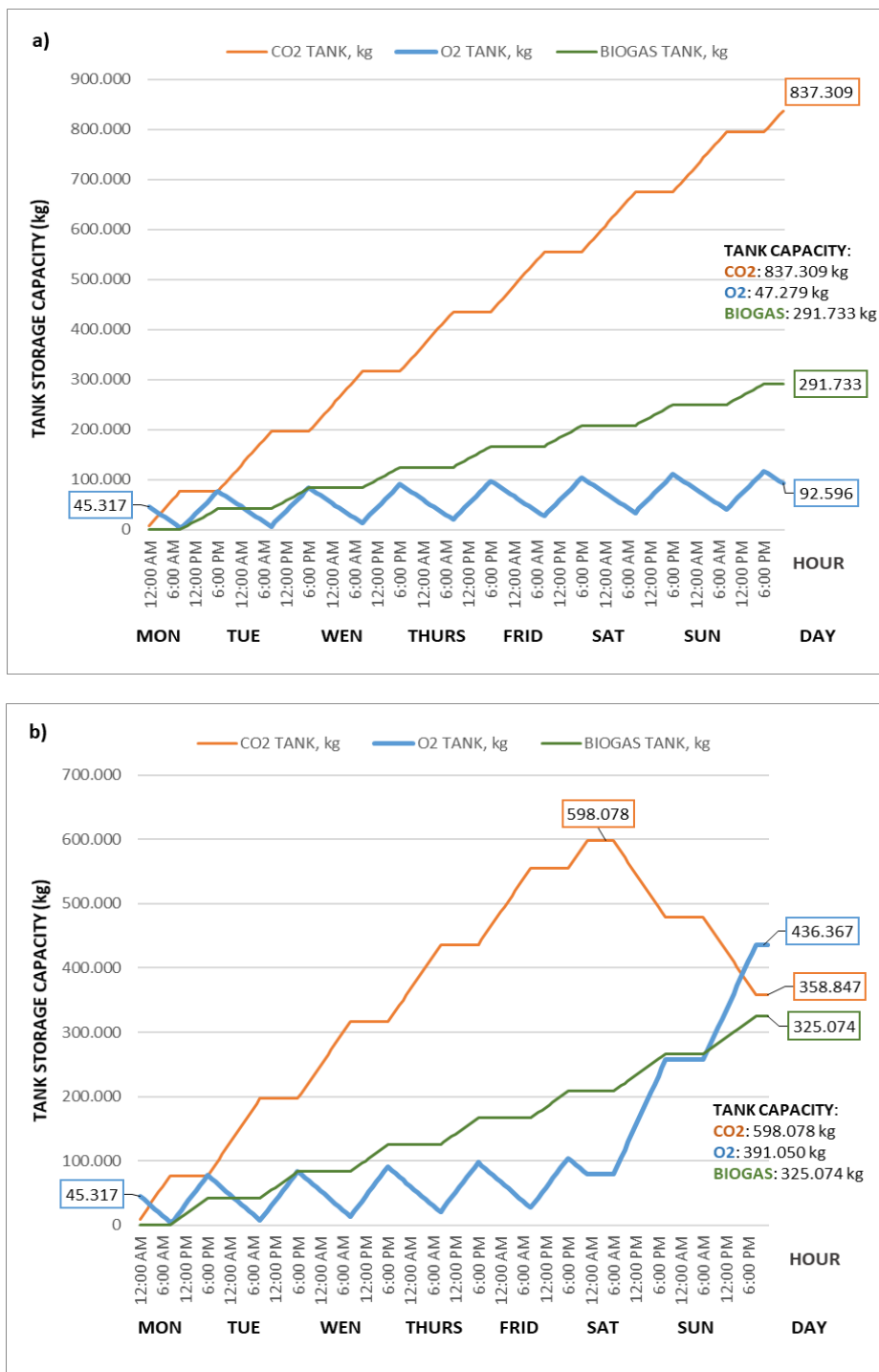


Fig. 7 a, b. Daily operation of the OxyMES system in the weekly operation cycle: a) Continuous operation from Monday to Sunday, 24 h/day for oxyboiler and 10 h/day for MES cell; b) Continuous operation from Monday to Friday, 24 h/day for Oxyboiler and 10 h/day for MES cell; from Saturday to Sunday, 14 h/day for MES cell (assuming higher surplus hours during the weekend). In each operation scenario a) and b), the minimum weekly storage capacity necessary for the CO₂, O₂ and biogas tanks is obtained according to the plant operation cycle.



445

446 **Fig. 8 a, b, c.** Tank storage capacity operating with a daily discharge cycle: a) continuous operation of 10
 447 hours of MES cell; b) discontinuous operation in two 5-hour periods of MES cell with two hours of lag
 448 between each period; c) discontinuous operation in two 5-hour periods of MES cell with three hours of lag
 449 between each period. The peak capacity value of the oxygen tank decreases as the offline period of the MES
 450 cell increases between operating periods.

451

452 From an application perspective in new decentralized energy models, the *OxyMES*
 453 schemes will better optimize their design and operation if they are integrated into networks
 454 connecting various industries, forming an *industrial hub*, so that they can transfer their
 455 surplus energy pre-carriers and carriers (CO₂, oxygen and biogas). In this way, the
 456 interconnection network itself will act as a buffer of the whole system and this would be a
 457 matter of advancing in the construction of a “*system of systems*” aimed at the effective
 458 implementation of circular and sustainable economy models [43].

459

460 3.2. Comparison of efficiency according to different scenarios of MES cells

461 For the same biogas production, four scenarios have been proposed in the sensitivity
 462 analysis of the efficiencies μ_{PtHeat_OxyMES} as a function of the cell potential (ΔV_{cell}), which is
 463 directly related to the energy consumed by the cell (Table 5). The four scenarios analysed
 464 are based on data and initial assumptions reported by different research groups mentioned

465 throughout the article. In this sense, it seeks to cover a reasonable range of *MES* cell
 466 operation in terms of the external potential to be applied. The most unfavourable potentials
 467 selected for the study are those that assume a greater electrical consumption in the cell:
 468 $\Delta V_{\text{cell}} = 3.5$ V, a case similar to that reported by Zhou et al. [41] and $\Delta V_{\text{cell}} = 2.8$ V by
 469 Gomez et al. [21], and represent the current state of the art (TRL3-4).

470 On the other hand, an optimistic scenario is proposed with lower cell overpotentials, and
 471 according to the trend in the results obtained by the different research teams, it is predicted
 472 that it can be achieved in the short term; in this case, the applied voltage would be $\Delta V_{\text{cell}} =$
 473 1.63 V, and assumption reached based on the lowest biocathode potential reported by
 474 Beese-Vasbender et al. [42] (-0.4 V vs. SHE). Finally, the fourth scenario simulates the
 475 theoretical minimum cell potential to be applied ($\Delta V_{\text{cell}} = \Delta V_{\text{theoretical cell}} = 1.23$ V) when
 476 considering no overpotentials losses; this scenario would represent the theoretical upper
 477 limit of the performance value that *OxyMES* could be aim for. In all scenarios, it is
 478 considered the same flow of oxycombustion gases entering to the *MES* cell.

479

	$\Delta V_{\text{cell}} =$ 1.23 V	$\Delta V_{\text{cell}} =$ 1.63 V	$\Delta V_{\text{cell}} =$ 2.8 V	$\Delta V_{\text{cell}} =$ 3.5 V
Chemical energy of inlet fuel fed to oxyboiler (LHV), MW_{th}	18.51	18.51	18.51	18.51
$\mu_{\text{Oxyboiler}}$, Oxyboiler efficiency (LHV), %	89.00	89.00	89.00	89.00
Q_b, heat absorbed by steam, MW_{th}	16.48	16.48	16.48	16.48
Chemical energy of biogas (LHV), MW_{th}	33.64	33.64	33.64	33.64
P_{e,MES}, MES electric consumption, MW_e	49.89	66.11	113.57	141.96
$\mu_{\text{PtG_MES}}$ MES efficiency, %	67.43	50.88	29.62	23.70
$\mu_{\text{PtGHeat_OxyMES}}$, OxyMES global efficiency, %	73.26	59.22	37.94	31.23

480 *Table 5. Summary of energy produced, consumed and efficiencies obtained for four ΔV_{cell} scenarios.*

481

482 Table 5 shows the influence on the performance of the electrical cell overpotentials [44]
 483 due to their direct relationship with the *MES* cell electrical consumption. Reducing these
 484 losses to a minimum is a fundamental objective to advance the development of *MES*
 485 technologies and their integration into different processes. The results obtained indicate
 486 achievable values of *power-to-gas* performance ($\mu_{\text{PtG_MES}}$) of 51% in the *MES* cell and 60%
 487 for the *OxyMES* integrated global system ($\mu_{\text{PtGHeat_OxyMES}}$). These data are in line with
 488 those reported for other *power-to-gas* schemes, such as [22, 45, 46]. This gives us an idea
 489 of the perspectives and applicability of the hybridization proposed in this work.

490

491 3.3. Comparison of *OxyMES* with conventional CO₂ capture plants

492 Another interesting advantage of *OxyMES* process is that the production of the oxygen
 493 necessary for the oxycombustion is carried out ‘*in situ*’ in the *MES* reactor. This represents
 494 a significant advantage in that it avoids the CAPEX and the OPEX of the oxygen

495 generation units used in conventional oxycombustion plants with CO₂ capture (ASU) [47].
 496 The ASU facilities assume between 5% and 6% penalties in the global energy efficiency of
 497 CO₂ capture plants [40, 48]. Similarly, the CO₂ compression and purification unit (CPU) is
 498 necessary for the delivery of CO₂ captured for transport and deep geological storage. In
 499 this case, the global efficiency penalty introduced by these units is between 4.5 % and 5%
 500 [40].

501 If we analyse the specific energy consumption W_{ASU} and W_{CPU} (kWh_e/kWh_{th}) of the ASU
 502 and CPU facilities that no longer need to be installed in the *OxyMES* scheme, expressed
 503 over the thermal energy of the steam produced in the oxyboiler, and compare them to the
 504 new units that need to be installed W_{MES} (*MES*), it can be done an approximate
 505 quantification of the relative energetic improvement against an oxycombustion plant with
 506 conventional CO₂ capture (see supplementary material). As a first option, it is proposed to
 507 store the biogas for subsequent delivery to the gas system, so this would require a prior
 508 treatment of upgrading to biomethane. For the calculation of $W_{Upgrading}$ (kWh_e/kWh_{th}), the
 509 specific energy consumption of the upgrading plant considered is 0.28 kWh_e/kg biogas
 510 (0.25 kWh_{th}/Nm³ biogas) [49, 50].

511 Table 6 shows the results of this comparative study, which is carried out on the scenario of
 512 $\Delta V_{cell} = 1.63$ V. In option A, the specific energy consumption of the *MES* cell (W_{MES}) has
 513 been included, while in options B and C, this consumption is considered negligible because
 514 it comes from surpluses of the electrical system. Option C reflects the improvement when
 515 the biogas is used as fuel for the oxyboiler ($W_{Upgrading} = 0$).

516 [Energy saved (E_s) + Energy produced (E_p)] vs. [Energy consumed (E_c)] [Eq. 12]

517

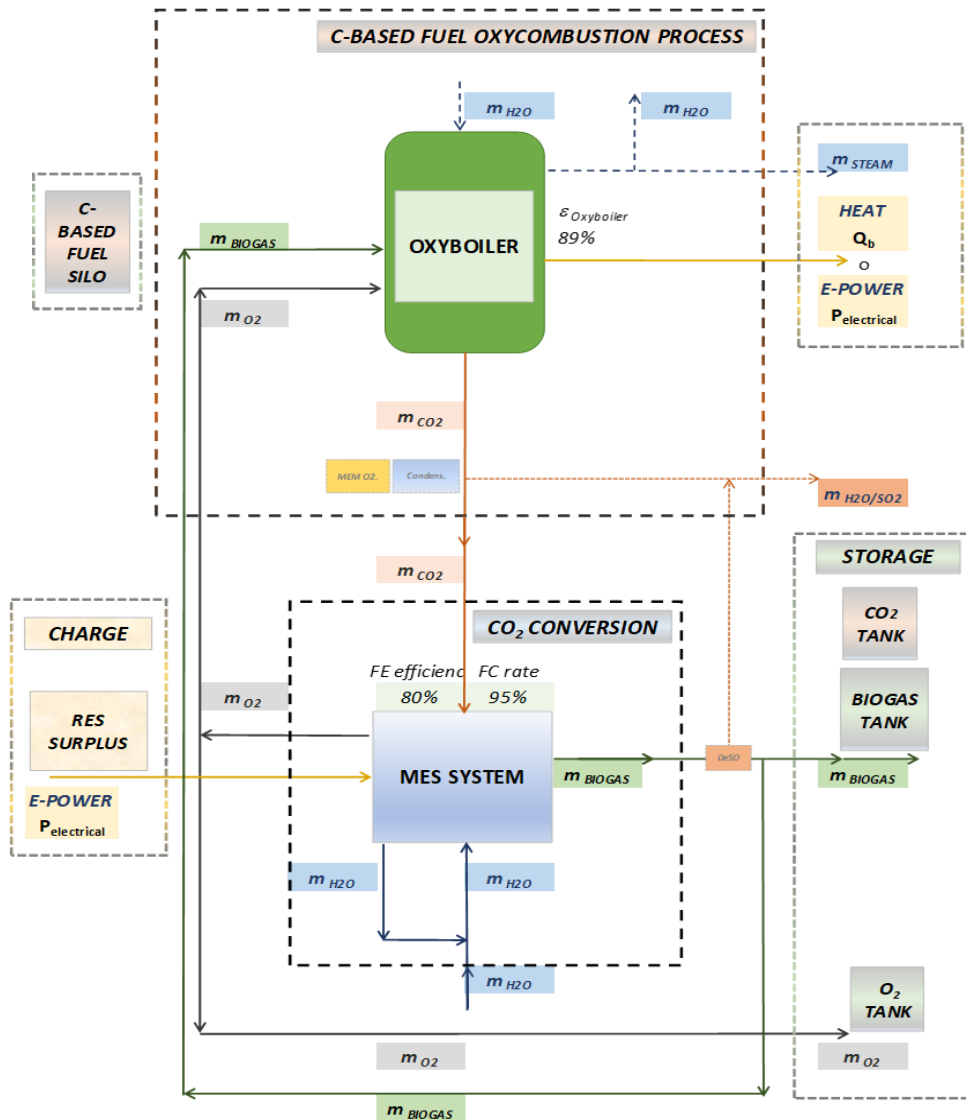
	W_{ASU} (kWh _e /kWh _{th} Q _b)	W_{CPU} (kWh _e /kWh _{th} Q _b)	W_{Biogas} (kWh _e /kWh _{th} Q _b)	W_{MES} (kWh _e /kWh _{th} Q _b)	$W_{Upgrading}$ (kWh _e /kWh _{th} Q _b)	ENERGY GAIN / LOSS (kWh _e /kWh _{th} Q _b)
IMPROVEMENT OPTION A: ASU & CPU avoided, MES and Upgrading biomethane to network						
<i>A.1</i>	0.0581	0.0511	0.7437	4.01244	0.0712	-3.2308
<i>A.2</i>	0.0581	0.0511	0.0000	4.01244	0.0712	-3.9745
IMPROVEMENT OPTION B: ASU & CPU avoided, MES 100% surplus RES and Upgrading biomethane to network						
<i>B.1</i>	0.0581	0.0511	0.7437	0.00000	0.0712	0.7816
<i>B.2</i>	0.0581	0.0511	0.0000	0.00000	0.0712	0.0379
IMPROVEMENT OPTION C: ASU & CPU avoided, MES 100% surplus RES, biogas for self-consumption						
<i>C.1</i>	0.0581	0.0511	0.7437	0.00000	0.00000	0.8528
<i>C.2</i>	0.0581	0.0511	0.0000	0.00000	0.00000	0.1091

518 **Table 6.** Relative specific consumption: results of the comparison with the reference plant (oxycombustion
 519 plant with CPU). Note: W_{Biogas} calculated considering a thermal to electric conversion efficiency of 36.43%
 520 (efficiency from a small-size CCGT plant). W_{ASU} calculated considering 190 kWh_e/tO₂ [22] and W_{CPU} , 120
 521 kWh_e/CO₂ [51].

522

523 The improvements obtained according to options B.1 and B.2 indicate that, depending on
 524 the chosen biogas upgrading technology, the avoided specific energy consumption of ASU
 525 and CPU (W_{ASU} and W_{CPU}) could alone compensate the specific energy consumption
 526 ($W_{Upgrading}$) of the upgraded installation, even without considering the thermal energy
 527 contained in the biogas (option B.2). The best energy improvement is achieved when
 528 upgrading is not required (options C.1 and C.2) replacing the original fossil fuel by the
 529 *MES* biogas for self-consumption purposes.

530



531

532 **Fig 9.** 100% self-sustaining “OxyMES” scheme, fed with the biogas produced in the MES (option C Table
 533 [6](#)).

534

535 After this preliminary comparative analysis, it is concluded that **an OxyMES system**
 536 **provides the energy storage function without energetically penalizing the process** if it
 537 is compared with an oxycombustion plant with conventional CO₂ capture. From the energy
 538 point of view, the best option for the implementation of the *OxyMES* scheme would be to

539 apply it as a measure to decarbonize an industry, switching the original fuel of the
540 oxycombustion boiler to the biogas generated in the *MES* cell (future study). This also
541 allows this industry to store RES surplus (see Figure 9) and consider new business models
542 that generate benefits derived from the energy storage market, which is currently
543 undergoing not only technical but also regulatory development [52, 53]. The second most
544 favourable option for the *OxyMES* implementation would be to use it as a system for
545 neutralizing the emissions of an industry recovering the CO₂ to biomethane for its network
546 injection, without having to substitute its primary fuel.

547 In any case, the *OxyMES* system has intrinsic advantages in that it produces biogas and
548 oxygen in a single piece of equipment ('*all-in-one*'), while other *power-to-gas* systems
549 require two intermediate steps with their corresponding equipment each (electrolyzer and
550 methanizer) [24, 54, 55]. Regardless, the production of oxygen in microbial systems
551 represents one of the greatest challenges facing *MES* technologies due to the high CAPEX
552 required to achieve stable membranes and anodes [56].

553

554 4. CONCLUSIONS

555 In this study, a novel scheme has been proposed for the storage of renewable electrical
556 energy surplus for its conversion to biogas through the hybridization of a microbial
557 electrosynthesis (*MES*) system with an industrial process operating in oxycombustion. The
558 *MES* cell is capable of treating the flue gases from the oxycombustion boiler and
559 converting them into biogas while providing it with the necessary oxygen for the
560 oxycombustion. The biogas can be stored and, later, purified to be discharged to the natural
561 gas network. This is an advantage over other *power-to-gas* schemes when valorizing CO₂
562 and producing oxygen in a single piece of equipment (*MES* cell).

563 The *OxyMES* system process has been simulated by integrating the gas flows from the
564 oxycombustion boiler to the *MES* cell and the biogas generated in it according to four
565 operating scenarios of the *MES* cell. These four cases are a function of the external applied
566 voltage to the electrodes: 1.23 V, 1.63 V, 2.8 V and 3.5 V. From the energy balance
567 analysis of the set, the *power-to-gas* efficiency in the *MES* cell is obtained, reaching a
568 value close to 51%; the global performance of the integrated *OxyMES* system resulted in
569 nearly 60%, for a cell with an FE 80%, FC 95% and $\Delta V_{\text{cell}} = 1.63$ V.

570 Another possible route for the use of the *MES*-cell biogas is its utilization within the
571 industrial process itself as a primary fuel, displacing the existing fossil fuel-based one. At
572 this point, the range of possible uses for self-consumption is extensive and will depend on
573 the characteristics of each industry. In this work, its self-consumption in the oxyboiler is
574 proposed so that it replaces the original fossil-fuel with a bio-renewable origin one. This
575 possibility is very interesting since it is possible to adapt the process to a circular economy
576 one and convert it into a *net-negative-emissions technology* system (*NET* system). With the
577 proper sizing of the O₂, biogas and CO₂ process tank system, it is possible to achieve 100%
578 autonomy and self-sustainability of the original industrial process. The influence on the
579 tank system design of the duration chosen for energy storage has been studied, that is, of

580 the operating cycles of the plant and of the daily charging and discharging cycles of the O₂,
581 biogas and CO₂ fluids. These fluids act as energy *pre-carriers* and *carriers*. It is seen how
582 for the new models of distributed generation with energy storage based on *power-to-gas*
583 systems, such as the proposed *OxyMES*, they are better positioned if they are integrated
584 into larger systems forming hubs of different industrial processes (*'system of systems'*
585 concept), forming local networks to transfer their surplus energy *pre-carriers* and adapted
586 to their environment.

587 Future studies could address the coupling of bottom cycles to the *OxyMES* process to
588 produce dispatchable electricity in a *power-to-power* scheme. This would enable the
589 industrial operator to participate in new electricity market models.

590 Finally, it is worth highlighting the great advantage of the *OxyMES* system, based on
591 microbial electrosynthesis, compared to other proposed *power-to-gas* solutions: it is an *all-*
592 *in-one* system, which means that it converts CO₂ to biogas and produces oxygen for oxy-
593 fuel combustion, all within a single system, with the consequent savings in CAPEX and
594 OPEX.

595

596 **CRedit authorship contribution statement**

597 **Ruth Diego:** Formal analysis, Investigation, Methodology, Writing- Original draft
598 preparation, Writing - Review & Editing, Visualization. **Antonio Morán:**
599 Conceptualization, Methodology, Supervision, Funding acquisition and Review. **Luis M.**
600 **Romeo:** Conceptualization, Methodology, Supervision and Review.

601

602 **Declaration of competing interest**

603 The authors declare that they have no known competing financial interests or personal
604 relationships that could have appeared to influence the work reported in this paper.

605 **Fundings:** This research was funded by the 'Ministerio de Ciencia e Innovación' project
606 ref: PID2020-115948RB-I00, co-financed by FEDER funds.

607 Part of the research that has given rise to these results has received funding from the
608 Seventh Framework Program of the European Community (FP7/2007-2013) under grant
609 agreement No. 268191.

610

611 **Appendix A. Supplementary material**

612 PDF file.

613

614 **NOMENCLATURE**

615 *Abbreviations*

616 ASU: Air Separation Unit

617 CAPEX: Capital Expenditures

618 CCS: CO₂ capture and storage
619 CO₂-to-CH₄ ratio = FC
620 CPU: Compression and Purification Unit
621 Current-to-methane efficiency = Faradaic efficiency = FE
622 kWh: Kilowatt hour
623 MEC: Microbial Electrolysis Cell
624 MES: Microbial Electrosynthesis System
625 MWh: Megawatt hour
626 MSW: Municipal Solid Waste
627 OPEX: Operational Expenditures
628 PEM: Proton Exchange Membrane
629 PtG: Power to Gas
630 PV: Photovoltaic
631 RES: Renewable Energy Sources
632
633 *Symbols*
634 F: Faraday constant, 96485 C/mol e⁻
635 HHV: Higher Heating Value [kJ/kg]
636 LHV: Lower Heating Value [kJ/kg]
637 M: molecular weight [g/mol]
638 m: mass flow [kg/h] or [t/h]
639 μ: efficiency (%)
640 NHE: Normal Hydrogen Electrode (V)
641 Q: thermal power [MW_{th}]
642 SHE: Standard Hydrogen Electrode (V)
643 ΔV: external applied voltage [V]
644 W: specific energy consumption [kWh_e/kWh_{th}]
645
646 *Subscripts:*
647 b: boiler
648 e: electricity

649 f: oxycombustion plant fuel (coal)

650 d.b.: dry basis

651 w.b.: wet basis

652 vol: by volume

653 th: thermal

654 wth: weight

655

656 REFERENCES

657 [1] IEA (2020), World Energy Outlook 2020, IEA, Paris,

658 <https://www.iea.org/reports/world-energy-outlook-2020> [accessed 30.01.22].

659 [2] Regulation (EU) 2021/1119 of the European Parliament and of the Council of 30 June
660 2021 establishing the framework for achieving climate neutrality and amending
661 Regulations (EC) No 401/2009 and (EU) 2018/1999 ('European Climate Law').
662 PE/27/2021/REV/1, <http://data.europa.eu/eli/reg/2021/1119/oj> [accessed 30.01.22].

663 [3] [Proposal for a DIRECTIVE OF THE EUROPEAN PARLIAMENT AND OF THE
664 COUNCIL amending Directive \(EU\) 2018/2001 of the European Parliament and of the
665 Council, Regulation \(EU\) 2018/1999 of the European Parliament and of the Council and
666 Directive 98/70/EC of the European Parliament and of the Council as regards the
667 promotion of energy from renewable sources, and repealing Council Directive \(EU\)
668 2015/652 - Progress report. ST 13670 2021 INI, \[https://eur-lex.europa.eu/legal-
669 content/EN/TXT/?uri=consil%3AST_13670_2021_INIT\]\(https://eur-lex.europa.eu/legal-content/EN/TXT/?uri=consil%3AST_13670_2021_INIT\) \[accessed 30.01.22\].](#)

670 [4] Directive (EU) 2018/2001 of the European Parliament and of the Council of 11
671 December 2018 on the promotion of the use of energy from renewable sources (Text with
672 EEA relevance) PE/48/2018/REV/1, <http://data.europa.eu/eli/dir/2018/2001/oj> [accessed
673 30.01.22].

674 [5] [REE. Reunión Extraordinaria del Grupo de Seguimiento de la planificación. Estudios
675 de prospectiva del sistema y necesidades para su operabilidad. 29/09/2020](#) [accessed
676 30.01.22].

677 [6] [California ISO \(CAISO\) Fast Facts: Impacts of renewable energy on grid operations.](#)
678 <http://www.caiso.com/informed/Pages/ManagingOversupply.aspx>. [accessed 30.01.22].

679 [7] [EASE-EERA. Joint EASE/EERA recommendations for a European Energy Storage
680 Technology Development Roadmap Towards 2030. and Joint EASE/EERA
681 recommendations ES Technology Development Roadmap 2030: Technical annex.](#)
682 [https://ease-storage.eu/publication/easeeera-energy-storage-technology-development-
683 roadmap-towards-2030/](https://ease-storage.eu/publication/easeeera-energy-storage-technology-development-
683 roadmap-towards-2030/) [accessed 30.01.22].

684 [8] Blanco H, Faaij A, A review at the role of storage in energy systems with a focus on
685 Power to Gas and long-term storage. Renewable and Sustainable, Energy Reviews,

686 Volume 81, Part 1, 2018, Pages 1049-1086, ISSN 1364-0321,
687 <https://doi.org/10.1016/j.rser.2017.07.062>.

688 [9] ETIP-SNET. White Paper. Sector Coupling: Concepts, State-of-the-art and
689 Perspectives. January 2020, [https://www.etip-snet.eu/etip_publication/sector-coupling-concepts-](https://www.etip-snet.eu/etip_publication/sector-coupling-concepts-state-art-perspectives/)
690 [state-art-perspectives/](https://www.etip-snet.eu/etip_publication/sector-coupling-concepts-state-art-perspectives/) [accessed 30.01.22].

691 [10] ETIP-SNET. Position Paper. Smart Sector Integration, towards an EU System of
692 Systems Building blocks, enablers, architectures, regulatory barriers, economic
693 assessment. July 2021, [https://www.etip-snet.eu/new-etip-snet-position-paper-smart-](https://www.etip-snet.eu/new-etip-snet-position-paper-smart-sector-integration-towards-eu-system-systems/)
694 [sector-integration-towards-eu-system-systems/](https://www.etip-snet.eu/new-etip-snet-position-paper-smart-sector-integration-towards-eu-system-systems/) [accessed 30.01.22].

695 [11] EASE Report. Energy Storage Applications Summary. June 2020, [https://ease-](https://ease-storage.eu/publication/energy-storage-applications-summary/)
696 [storage.eu/publication/energy-storage-applications-summary/](https://ease-storage.eu/publication/energy-storage-applications-summary/) [accessed 30.01.22].

697 [12] Ritchie H, Roser M. CO₂ and Greenhouse Gas Emissions. Published online at
698 OurWorldInData.org. 2020. Retrieved from: 'https://ourworldindata.org/co2-and-other-
699 greenhouse-gas-emissions' [Online Resource], [https://ourworldindata.org/emissions-by-](https://ourworldindata.org/emissions-by-sector)
700 [sector](https://ourworldindata.org/emissions-by-sector) [accessed 30.01.22].

701 [13] Communication from the Commission to the European Parliament, the Council, The
702 European Economic and Social Committee and the Committee of the Regions: Powering a
703 climate-neutral economy: An EU Strategy for Energy System Integration. COM/2020/299
704 final. 08/07/2020, [https://eur-lex.europa.eu/legal-](https://eur-lex.europa.eu/legal-content/EN/ALL/?uri=COM:2020:299:FIN)
705 [content/EN/ALL/?uri=COM:2020:299:FIN](https://eur-lex.europa.eu/legal-content/EN/ALL/?uri=COM:2020:299:FIN) [accessed 30.01.22].

706 [14] Olah, G. A, Goepfert A, Surya Prakash G. K. Beyond Oil and Gas: The Methanol
707 Economy, 3rd ed., 2018. Wiley-VCH, Weinheim, Germany. ISBN: 978-3-527-80567-9.

708 [15] EASE- Energy Storage for a Decarbonised Europe by 2050. Brussels, November
709 2019, <https://ease-storage.eu/publication/decarbonised-europe-2050/> [accessed 30.01.22].

710 [16] Bajracharya S, Sharma M, Mohanakrishna G, Dominguez Benneton X, Strik D PBTB,
711 Sarma P M, Pant D, An overview on emerging bioelectrochemical systems (BESs):
712 Technology for sustainable electricity, waste remediation, resource recovery, chemical
713 production and beyond. Renewable Energy, Volume 98, 2016, Pages 153-170, ISSN 0960-
714 1481, <https://doi.org/10.1016/j.renene.2016.03.002>.

715 [17] Bajracharya S, Srikanth S, Mohanakrishna G, Zacharia R, Strik D PBTB, Pant D.
716 Biotransformation of carbon dioxide in bioelectrochemical systems: State of the art and
717 future prospects. Journal of Power Sources. 2017; 356:256-273,
718 <https://doi.org/10.1016/j.jpowsour.2017.04.024>

719 [18] Salimijazi F, Kim J, Schmitz A.M, Grenville R., Bocarsly A, Barstow B. Constraints
720 on the efficiency of engineered electromicrobial production. Joule 4, 2101–2130. 2020,
721 <https://doi.org/10.1016/j.joule.2020.08.010>.

722 [19] Villano M, Aulenta F, Ciucci C, Ferri T, Giuliano A, Majone M. Bioelectrochemical
723 reduction of CO₂ to CH₄ via direct and indirect extracellular electron transfer by a

724 hydrogenophilic methanogenic culture. *Bioresource technology*. 2010 May;101(9): 3085-
725 90, <https://doi.org/10.1016/j.biortech.2009.12.077>

726 [20] Cheng S, Xing D, Call DF, Logan BE. Direct biological conversion of electrical
727 current into methane by electromethanogenesis. *Environ Sci Technol*. 2009 May
728 15;43(10): 3953-8, <https://doi.org/10.1021/es803531g>

729 [21] Gomez Vidales A, Omanovic S, Tartakovsky B. Combined energy storage and
730 methane bioelectrosynthesis from carbon dioxide in a microbial electrosynthesis system.
731 2019, <https://doi.org/10.1016/j.biteb.2019.100302>

732 [22] Bailera M, Lisbona P, Romeo L M. Power to gas-oxyfuel boiler hybrid systems. 2015.
733 *International Journal of Hydrogen Energy*, Volume 40, Issue 32, 2015, Pages 10168-
734 10175, ISSN 0360-3199, <https://doi.org/10.1016/j.ijhydene.2015.06.074>

735 [23] Bailera M, Kezibri N, Romeo L M, Espatolero S, Lisbona P, Bouallou C. Future
736 applications of hydrogen production and CO2 utilization for energy storage: Hybrid Power
737 to Gas-Oxycombustion power plants. *International Journal of Hydrogen Energy*, Volume
738 42, Issue 19, 2017, Pages 13625-13632, ISSN 0360-3199,
739 <https://doi.org/10.1016/j.ijhydene.2017.02.123>

740 [24] Faria D G, Carvalho M MO, Neto M RV, de Paula E C, Cardoso M, Vakkilainen E K.
741 Integrating oxy-fuel combustion and power-to-gas in the cement industry: A process
742 modeling and simulation study, *International Journal of Greenhouse Gas Control*, Volume
743 114, 2022, 103602, ISSN 1750-5836, <https://doi.org/10.1016/j.ijggc.2022.103602>

744 [25] Rispoli A L, Verdone N, Vilardi G. Green fuel production by coupling plastic waste
745 oxy-combustion and PtG technologies: Economic, energy, exergy and CO2-cycle analysis,
746 *Fuel Processing Technology*, Volume 221, 2021, 106922, ISSN 0378-3820.
747 <https://doi.org/10.1016/j.fuproc.2021.106922>

748 [26] Bailera M, Lisbona P, Romeo LM, Espatolero S. Power to Gas projects review: lab,
749 pilot and demo plants for storing renewable energy and CO2. *Renew Sustain Energy Rev*
750 2017; 69:292e312, <https://doi.org/10.1016/j.rser.2016.11.130>

751 [27] Aryal N, Kvist T, Amman F, Pant D, Ottosen L DM. An overview of microbial biogas
752 enrichment. *Bioresource Technology*, Volume 264, 2018, Pages 359-369, ISSN 0960-
753 8524, <https://doi.org/10.1016/j.biortech.2018.06.013>

754 [28] Lockwood, T. IEA Clean Coal Centre Report. Developments in oxyfuel combustion
755 of coal. ISBN: 978-92-9029-561-7. 2014.

756 [29] Stanger R, Wall T, Spörl R, Paneru M, Grathwohl S, Weidmann M, Scheffknecht G,
757 McDonald D, Myöhänen K, Ritvanen J, Rahiala S, Hyppänen T, Mletzko J, Kather A,
758 Santos S. Oxyfuel combustion for CO2 capture in power plants. *International Journal of*
759 *Greenhouse Gas Control*. 2015, <https://10.1016/j.ijggc.2015.06.010>

760 [30] [BOE-A-2018-14557](https://www.boe.es/boe-2018-14557) Resolución de 8 de octubre de 2018, de la Dirección General de
761 Política Energética y Minas, por la que se modifican las normas de gestión técnica del

762 sistema NGTS-06, NGTS-07 y los protocolos de detalle PD-01 y PD-02. Ministerio para la
763 Transición Ecológica; 2018.

764 [31] Diego R; López C, Navarrete B, Coca T, López LA. CIUDEN PC Boiler
765 Technological Development in Power Generation. 2nd IEAGHG Oxyfuel Combustion
766 Conference, 12-16/09/2011, Yeppoon, QLD, Australia, 2011.

767 [32] FP7-ENERGY European Commission Funding Project. Reliable and Efficient
768 Combustion of Oxygen/Coal/Recycled Flue Gas Mixtures (RELCOM Project):
769 <https://cordis.europa.eu/project/id/268191> [accessed 30.01.22].

770 [33] Geppert F, Liu D, van Eerten-Jansen M, Weidner E, Buisman C, Ter Heijne A.
771 Bioelectrochemical Power-to-Gas: State of the Art and Future Perspectives. Trends
772 Biotechnol. 2016 Nov;34(11):879-894, <https://doi.org/10.1016/j.tibtech.2016.08.010>

773 [34] Mateos R, Escapa A, San-Martín MI, De Wever H, Sotres A, Pant D. Long-term open
774 circuit microbial electrosynthesis system promotes methanogenesis. Journal of Energy
775 Chemistry, Volume 41, 2020, Pages 3-6, ISSN 2095-4956,
776 <https://doi.org/10.1016/j.jechem.2019.04.020>

777 [35] Villano M, Ralo C, Zeppilli M, Aulenta F, Majone M. Influence of the set anode
778 potential on the performance and internal energy losses of a methane-producing microbial
779 electrolysis cell. Bioelectrochemistry. 2016 Feb; 107:1-6,
780 <https://doi.org/10.1016/j.bioelechem.2015.07.008>

781 [36] Batlle-Vilanova P, Dissertation PhD: Bioelectrochemical transformation of carbon
782 dioxide to target compounds through microbial electrosynthesis. University of Girona.
783 2016, <https://dugi-doc.udg.edu/handle/10256/13415>

784 [37] Pelaz G, Carrillo-Peña D, Morán A, Escapa A. Electromethanogenesis at medium-low
785 temperatures: Impact on performance and sources of variability, Fuel, Volume 310, Part A,
786 2022, 122336, ISSN 0016-2361, <https://doi.org/10.1016/j.fuel.2021.122336>

787 [38] Spiess S, Sasiain A, Waldmann N, Neuhauser E, Loibner A P, Kieberger N,
788 Haberbauer M. Bioelectrochemical Methanation of CO₂ from Untreated Steel Mill Gas.
789 Proceeding from 5th European Meeting of the International Society for Microbial
790 Electrochemistry and Technology (ISMET) September 2021. <https://euismet2021.eu/>

791 [39] California ISO (CAISO). The Renewables Watch Report: Wind and Solar Curtailment
792 December 29, 2021. [http://www.caiso.com/Documents/Wind_SolarReal-
793 TimeDispatchCurtailmentReportDec29_2021.pdf](http://www.caiso.com/Documents/Wind_SolarReal-TimeDispatchCurtailmentReportDec29_2021.pdf) [accessed 30.01.22].

794 [40] Escudero A I, Espatolero S, Romeo L M, Lara Y, Paufigue C, Lesort A-L, Liszka. M
795 Minimization of CO₂ capture energy penalty in second generation oxy-fuel power plant.
796 Applied Thermal Engineering, Volume 103, 2016, Pages 274-281, ISSN 1359-4311,
797 <https://doi.org/10.1016/j.applthermaleng.2016.04.116>

798 [41] Zhou H, Xing D, Xu M, Su Y, Ma, J, Angelidaki I, Zhang Y. Optimization of a newly
799 developed electromethanogenesis for the highest record of methane production. Journal of
800 Hazardous Materials, Volume 407, 2021, 124363, ISSN 0304-3894,

801 <https://doi.org/10.1016/j.jhazmat.2020.124363>

802 [42] Beese-Vasbender PF, Grote JP, Garrelfs J, Stratmann M, Mayrhofer KJ. Selective
803 microbial electrosynthesis of methane by a pure culture of a marine lithoautotrophic
804 archaeon. *Bioelectrochemistry* (Amsterdam, Netherlands), Volume 102, 2015, pages 50–
805 55, ISSN 1567-5394, <https://doi.org/10.1016/j.bioelechem.2014.11.004>

806 [43] ETIP SNET Report. VISION 2050 Integrating Smart Networks for the Energy
807 Transition: Serving Society and Protecting the Environment. [https://www.etip-snet.eu/etip-](https://www.etip-snet.eu/etip-snet-vision-2050/)
808 [snet-vision-2050/](https://www.etip-snet.eu/etip-snet-vision-2050/) [accessed 30.01.22].

809 [44] Chen S, Patil S A, Brown R K, Schröder U. Strategies for optimizing the power output
810 of microbial fuel cells: Transitioning from fundamental studies to practical
811 implementation. *Applied Energy*, Volumes 233–234, 2019, Pages 15-28, ISSN 0306-2619,
812 <https://doi.org/10.1016/j.apenergy.2018.10.015>

813 [45] Thema M, Bauer F, Sterner M. Power-to-Gas: Electrolysis and methanation status
814 review. *Renewable and Sustainable Energy Reviews*, Volume 112, 2019, Pages 775-787,
815 ISSN 1364-0321, <https://doi.org/10.1016/j.rser.2019.06.030>

816 [46] Frank E, Gorre J, Ruoss F, Friedl M J. Calculation and analysis of efficiencies and
817 annual performances of Power-to-Gas systems. *Applied Energy*, Volume 218, 2018, Pages
818 217-231, ISSN 0306-2619, <https://doi.org/10.1016/j.apenergy.2018.02.105>

819 [47] Nuortimo K, Eriksson T, Kuivalainen R, Härkönen J, Haapasalo H, Hyppänen T.
820 Tackling boundaries of CCS in market deployment of second-generation oxy-fuel
821 technology. *Clean Energy*, Volume 2, Issue 1, 2018, Pages 72–81,
822 <https://doi.org/10.1093/ce/zky002>

823 [48] Perrin N, Dubettier R, Lockwood F, Tranier J-P, Bourhy-Weber C, Terrien P.
824 Oxycombustion for coal power plants: Advantages, solutions and Projects. *Applied*
825 *Thermal Engineering*, Volume 74, 2015, Pages 75-82, ISSN 1359-4311,
826 <https://doi.org/10.1016/j.applthermaleng.2014.03.074>

827 [49] Bauer F, Hulteberg C, Persson T, Tamm D. (2013). Biogas upgrading - Review of
828 commercial technologies. (SGC Rapport; Vol. 270). Svenskt Gastekniskt Center AB.
829 Retrieved from: <http://www.sgc.se/ckfinder/userfiles/files/SGC270.pdf>

830 [50] Gray N, O'Shea R, Smyth B, Lens P NL, Murphy J D. What is the energy balance of
831 electrofuels produced through power-to-fuel integration with biogas facilities?, *Renewable*
832 *and Sustainable Energy Reviews*, Volume 155, 2022, 111886, ISSN 1364-0321,
833 <https://doi.org/10.1016/j.rser.2021.111886>

834 [51] Espatolero S, Romeo LM. Optimization of oxygen-based CFBC technology with CO₂
835 capture. *Energy Procedia*, 2017, Volume 114, pages 581-588.

836 [52] EASE. The Ancillary Services Report. 2021. Available on-line: [https://ease-](https://ease-storage.eu/publication/ancillary-services/)
837 [storage.eu/publication/ancillary-services/](https://ease-storage.eu/publication/ancillary-services/) [accessed 30.01.22].

838 [53] [Hillberg, Emil & zegers, antony & herndler, barbara & Wong, Steven & pompee, jean](#)
839 [& Bourmaud, Jean-Yves & lehnhoff, sebastian & migliavacca, gianluigi & Uhlen, Kjetil &](#)

- 840 [Oleinikova, I. & Phil, Hjalmar & Norström, Markus & Persson, Mattias & Rossi, Joni &](#)
841 [Beccuti, Giovanni. \(2019\). Flexibility needs in the future power system. Doi:](#)
842 [10.13140/RG.2.2.22580.71047. https://www.iea-igsaw.org/flexibility-in-future-power-](#)
843 [systems/](#) [accessed 30.01.22].
- 844 [54] Schorn F, Lohse D, Samsun R C, Peters R, Stolten D. The biogas-oxfuel process as a
845 carbon source for power-to-fuel synthesis: Enhancing availability while reducing
846 separation effort. Journal of CO2 Utilization, Volume 45, 2021, 101410, ISSN 2212-9820,
847 <https://doi.org/10.1016/j.jcou.2020.101410>
- 848 [55] Ipsakis D, Varvoutis G, Lampropoulos A, Papaefthimiou S, Marnellos G E,
849 Konsolakis M. Techno-economic assessment of industrially-captured CO2 upgrade to
850 synthetic natural gas by means of renewable hydrogen, Renewable Energy, Volume 179,
851 2021, Pages 1884-1896, ISSN 0960-1481, <https://doi.org/10.1016/j.renene.2021.07.109>
- 852 [56] PrévotEAU A, Carvajal-Arroyo JM, Ganigué R, Rabaey K. (2020). Microbial
853 electrosynthesis from CO2: forever a promise? Current Opinion in Biotechnology, Volume
854 62, 2020, Pages 48-57, ISSN 0958-1669, <https://doi.org/10.1016/j.copbio.2019.08.014>